Appl Magn Reson (2016) 47:159–174
DOI 10.1007/s00723-015-0755-3

Applied
Magnetic Resonance

Prediction of Indolent Breast Cancer with Favorable Prognostic Factors by Metabolic Profiling Using In Vivo and Ex Vivo MR Metabolomics

Hee Jung Shin[1] · Suhkmann Kim[2] · Hyeon-Man Baek[3] · Dahye Yoon[2] · Siwon Kim[2] · Joo Hee Cha[1] · Hak Hee Kim[1]

Received: 1 July 2015 / Revised: 17 September 2015 / Published online: 8 January 2016

Abstract To evaluate whether metabolic profiles obtained using high-resolution magic angle spinning magnetic resonance spectroscopy (HR MAS MRS) and total choline-containing compound (tCho) on in vivo MRS could predict indolent tumors based on highly favorable prognostic factors. We analyzed 50 frozen tissue samples from 50 patients (mean 46.4 years, range 29–72 years) with breast cancer using HR MAS MRS. In vivo single-voxel MRS analyses were also performed on these patients preoperatively. We defined estrogen receptor (ER)-positive tumors with a low histological grade, low Ki-67-positivity (<14 %), and negative lymph node metastases as an indolent tumor. By univariate analysis, metabolic profiles on HR MAS MRS and tCho on in vivo MRS were compared according to dichotomized pathological parameters using the Mann–Whitney test. By multivariate analysis, orthogonal projections to latent structure-discriminant analysis (OPLS-DA) were performed to differentiate groups with different prognostic pathological parameters. A total of 6 indolent tumors (12 %) and 44 non-indolent tumors (88 %) were studied. By univariate analysis, tumors without recurrence showed significantly higher Tau and Cr values than those with recurrence ($P = 0.041$, respectively). By multivariate analysis, an OPLS-DA model showed sensitivities of 100, 77, and 82 % and specificities of 68, 100, and 96 % for the prediction of indolent tumors, tumors with recurrence, and tumors with lymph node metastases, respectively. By univariate analysis of in vivo MRS, tumors without recurrence showed significantly

✉ Hee Jung Shin
docshin@amc.seoul.kr

[1] Department of Radiology and Research Institute of Radiology, Asan Medical Center, College of Medicine, University of Ulsan, 88 Olympic-ro, 43-gil, Songpa-gu, Seoul 138-736, South Korea

[2] Department of Chemistry, Chemistry Institute for Functional Materials, Pusan National University, Busan 609-735, South Korea

[3] Department of Bio-Analytical Science, University of Science and Technology, 162 Yeongudanji-ro, Ochang-eup, Cheongwon-gun, Chungbuk 363-883, South Korea

higher values of tCho than those with recurrence ($P = 0.043$ and 0.035). Several metabolites of Gly, Lac, Tau, Cr, GPC, and Cho on HR MAS MRS could be potential candidate biomarkers for predicting indolent tumors, tumors with early recurrence, and lymph node metastases. Metabolite profiling using HR MAS MRS might enable the prediction of breast cancer prognoses, especially for ER-positive tumors.

1 Introduction

Breast cancer is a heterogeneous disease that is associated with variable clinical and pathological factors that influence patient outcomes [1]. Prognoses of breast cancer patients vary depending upon the aggressiveness and metastatic status of the disease [2]. Cancer cells have altered metabolism compared with normal cells, including high glucose uptake and increased lactate production, and an altered metabolic status has been recently identified as a hallmark of cancer [3, 4]. Detailed analyses of cancer tissues can provide new biological data that are important for optimizing individual patient management [5]. Many studies have shown that metabolic profiling using MR spectroscopy represents a promising tool for cancer diagnosis and treatment monitoring [5–7].

High-resolution magic angle spinning (HR MAS) magnetic resonance spectroscopy (MRS) allows for quantitative measurements of metabolites with minimal pretreatment preparation [5]. HR MAS MRS has a high degree of reproducibility and a non-destructive nature, which allows specimens to be evaluated by histopathology, gene expression profiling, or other methods after spectral analysis. Such approaches allow direct comparisons to be made between spectral and morphological characteristics [4, 5, 8]. More than 30 metabolites have been identified in breast tissue using HR MAS MRS [10]. Previous studies have shown that the metabolite profiles of breast cancer tissues correlate with different prognostic factors, including hormone receptor status, histological grade, and lymphatic spread [9–11]. In vivo single-voxel MRS may be a promising diagnostic tool for breast cancer that has high sensitivity (92 %) and low specificity (78 %) [12–14]. Increased total choline-containing compound (tCho) is regarded as a marker for elevated cell proliferation rates in breast cancer, which may be associated with tumor aggressiveness [13]. Several studies have shown that tCho peaks on in vivo MRS can be correlated with prognostic factors of breast cancer [15, 16]. MR metabolomics could provide prognostic information that adds to current clinical and pathological assessments.

An immunohistochemical (IHC) profile based on estrogen receptor (ER), progesterone receptor (PR), and HER2 expression is the most frequently used molecular marker system, and breast cancers can be classified into subgroups with different prognoses [17]. These IHC subtypes roughly correspond to the molecular subtypes of luminal, HER2-positive, and basal-like tumors [18]. A four-marker IHC panel (ER, PR, HER-2, and Ki67) has the potential to guide adjuvant therapy and to allow for surrogate definitions of intrinsic subtypes of breast cancer [19, 20]. One of the most important clinical questions in breast cancer treatment is how subsets of

patients among ER-positive and node-negative breast cancer patients can be safely spared adjuvant chemotherapy [21]. Oncotype DX is most frequently used for making decisions regarding the advisability of adjuvant chemotherapy for such patients [22], but it can be prohibitively expensive. To the best of our knowledge, few studies have examined metabolic biomarkers using in vivo and ex vivo MRS to differentiate indolent tumors from other types of tumor. Therefore, our current study aimed to investigate whether the metabolic profiles on HR MAS MRS and tCho on in vivo MRS could predict indolent tumors with favorable prognostic factors (node-negative, ER-positive tumors with a low histological grade (HG) and low Ki67 <14 %).

2 Materials and Methods

2.1 Patient Selection

This retrospective study was approved by our institutional review board. Written informed consent for biobank storage was obtained from all patients at the time of surgery. Subjects were identified from a retrospective review of breast cancer tissue biobank samples available at our institution. The biospecimens and data used in this study were provided by the Asan Bio-Resource Center, Korea Biobank Network. This current study series consisted of 50 patients (mean 46.4 years, range 29–72 years) diagnosed with breast cancer between July 2009 and May 2011. Only patients who underwent preoperative in vivo MRS were included, and none of the patients had received neoadjuvant treatment prior to surgery. Tissue samples were frozen in liquid nitrogen immediately after surgical removal of the tumor and were stored until use in experiments. A single pathologist with 20 years of experience in breast pathology meticulously attempted to exclude non-tumorous breast parenchyma or fat tissues based on the macroscopic findings of tissue samples.

2.2 Pathology

Pathological findings at definitive surgery served as the reference standard. A single pathologist interpreted the histopathological specimens. Data regarding the histological grade, ER, PR, HER-2/neu, HER-1, CK5/6, and lymph node metastases were obtained. ER- or PR-positivity was scored using an Allred score [23], which was a semiquantitative system that considered the proportion of positive cells (scored on a 0–5 scale) and staining intensity (scored on a 0–3 scale). The proportions and intensity scores were then summed to produce total scores of 0 or 2 through 8. The tumor was considered to be positive for ER or PR if the Allred score was >2. The HER-2/neu status was initially determined by immunohistochemical staining (IHC) and scored as 0 through 3; tissues scored as 2 were further evaluated by fluorescent in situ hybridization. We classified node-negative, ER-positive tumors with a low histological grade and low Ki67 expression (<14 %) as indolent tumors [20].

2.3 Ex Vivo HR MAS MRS Experiments

Tissue samples were defrosted at room temperature immediately prior to analysis. HR MAS MRS was performed on a nuclear magnetic resonance (NMR) spectrometer (Varian Unity-Inova; Varian Inc., Palo Alto, CA, USA) operating at a proton NMR frequency of 600 MHz (11.7 T) and equipped with a gHXnano probe. Frozen samples were thawed in the NMR laboratory, weighed, and placed in an HR MAS nano-probe®. The total sample weight was 25 mg. Samples were placed in the cell with the remaining volume filled with D_2O-containing 2 mM trimethylsilyl propionic acid (TSP) and were analyzed using a Carr–Purcell–Meiboom–Gill (CPMG) pulse sequence (recycle delay–90–(τ–180–τ)n-acquisition where $\tau = 400$ μs and $n = 80$) to impose a T2 filter. Acquisition parameters were as follows: 19.231 K complex data points, 9615.4 Hz sweep width, 2 s acquisition time, 1.0 s relaxation delay, 1.5 s saturation time, and 4.0 ms inter-pulse delay. Inter-pulse delay means tau value, which represents delay between first and second pulse on CPMG pulse sequence.

Spectra were processed and analyzed using ACD software (Advanced Chemistry Development, Toronto, ON, Canada). Post-processing consisted of Fourier transformation, phasing, and baseline correction. Chemical shifts were referenced in relation to the creatine (Cr) signal at 3.04 ppm. Spectral regions from 1.47 to 3.60 ppm [acetate (Ace), alanine (Ala), arginine (Arg), aspartate (Asp), creatine (Cr), creatinine (Cre), free choline (Cho), cysteine (Cys), formate (For), fumarate (Fum), glucose (Glu), glutamate (Glm), glutamine (Gln), histidine (His), isoleucine (Ile), lactate (Lac), leucine (Leu), lysine (Lys), methionine (Met), phosphocholine (PC), glycerophosphocholine (GPC), myo-inositol (m-Ins), taurine (Tau), proline (Pro), ribose (Rib), serine (Ser), succinate (Suc), phenylalanine (Phe), valine (Val), tyrosine (Tys), and glycine (Gly)] were selected for quantification (Fig. 1). The peak amplitudes of metabolites were measured by fitting a Voigt line-shape function. The integration values were normalized to both the number of contributing protons per molecule and tissue weight. Quantification was performed by comparing the integrated TSP signal to the signal of interest in the tumor spectrum after eretic correction. Absolute concentrations were recorded as μmol/g wet-weight.

2.4 In Vivo Single-Voxel Proton MR Spectroscopy

An in vivo single-voxel proton MRS was performed on a 1.5 T MR scanner (Magnetom Avanto, Siemens Medical Solutions, Erlangen, Germany). Automated parameter optimization was performed. To minimize eddy currents and maximize the water signal, a localized MRS was first performed with water suppression to adjust the gradients. The gradient tuning and stability were verified by pre-localizing a volume of interest (VOI) in a subject. A semiautomatic shimming adjustment was performed to reach a full width at half maximum (FWHM) of the unsuppressed water peak lower than 25 Hz as a quality parameter of the MR signal. Proton MRS spectra were acquired using the following technical parameters: TR = 1500 ms, TE = 135 ms, 128 acquisitions, spectral width = 1000 Hz, and 1024 data points. The MRS scan time was 3 min 18 s. The volume of interest (VOI)

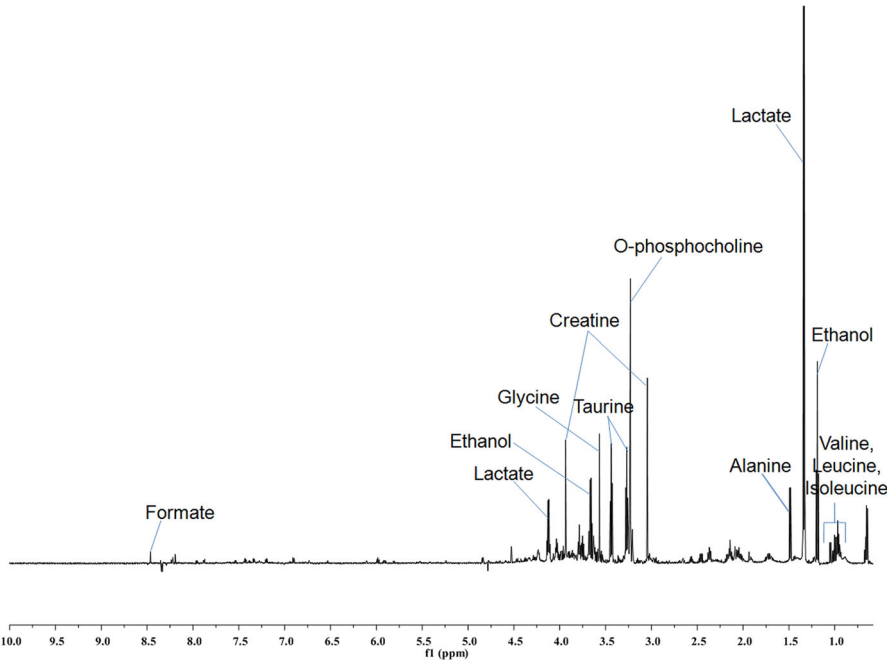

Fig. 1 A 61-year-old patient with invasive ductal carcinoma and without recurrence. The HR MAS MR spectrum shows peaks for lactate at 1.32 and 4.11 ppm, in addition to increased signals from glycine, taurine, valine, isoleucine, leucine, and creatine. The patient had a pathologically confirmed, node-negative, ER-positive tumor with a low histological grade, no Ki67 expression, and negative HER2 status

of a rectangular box was positioned to encompass each enhancing lesion, excluding nonenhancing parenchyma or surrounding fat as much as possible. The jMRUI software package [24] was used for time-domain analysis. The analysis method used has been described in a previous study [16]. After August 2010, we obtained an absolute tCho concentration (mmol/kg), whereas we obtained only semiquantitative measurements of tCho [tCho peak integral and tCho signal-to-noise ratio (SNR)] before July 2010.

2.5 Statistical Analysis

Clinical and pathological characteristics of patients were recorded from a review of patient medical records (summarized in Table 1). Absolute metabolite concentrations acquired by HR MAS MRS were evaluated. On in vivo MRS, the tCho peak integral, tCho SNR, and tCho concentration were also assessed. Statistical analysis was performed using SPSS for Windows 19.0 (SPSS, Chicago, IL, USA). By univariate analysis, data were dichotomized according to pathological parameters. We defined a node-negative, ER-positive tumor with a low histological grade and low Ki67 <14 % as an indolent tumor and others were classified as non-indolent tumors [20]. We also compared metabolic profiles according to LN metastasis and

recurrence. We used the Mann–Whitney test because the data did not show a normal distribution on the Kolmogorov–Smirnov test ($P < 0.05$). Two-tailed statistical tests were always used, and findings with a P value less than 0.05 were considered statistically significant.

For multivariate analysis, ^{1}H NMR spectra were binned using Chenomx NMR Suite 7.1 software (Spectral database; Edmonton, AB, Canada). Spectra were normalized to the total area. The spectral region between δ 0.5–10 ppm was binned with 0.001 ppm. The water region from 4.6 to 4.9 ppm and ethanol peaks (1.15–1.20, 3.6–3.7 ppm) were excluded prior to analysis. Matlab (MathWorks, Natick, MA, USA), SIMCA-P 11.0 (Umetrics, Sweden), and Excel (Microsoft, Seattle, WA, USA) software were used. Orthogonal projection to latent structure-

Table 1 Clinicopathological characteristics of the 50 breast tumors analyzed in this study based on indolence

Characteristics	Indolent tumor ($n = 6$)	Non-indolent tumor ($n = 44$)	P value
Age, years, mean (range)	43.2 (35–62)	48.1 (29–72)	0.333
Histological subtype			0.449
Invasive ductal carcinoma	5 (83)	40 (91)	
Invasive lobular carcinoma	0 (0)	2 (4.5)	
Mucinous carcinoma or others	1 (17)	2 (4.5)	
Histologic grade			0.023*
Low or intermediate	6 (100)	20 (45)	
High	0 (0)	24 (55)	
HER-2/neu			0.167
Negative	6 (100)	30 (68)	
Positive	0 (0)	25 (32)	
HER-1			0.327
Negative	6 (100)	34 (77)	
Positive	0 (0)	10 (23)	
P53			0.023*
Negative	6 (100)	20 (45)	
Positive	0 (0)	24 (55)	
CK6/7			0.556
Negative	5 (83)	39 (89)	
Positive	1 (17)	5 (11)	
Extensive intraductal component			0.601
Negative	4 (67)	35 (80)	
Positive	2 (33)	9 (20)	
Lymphovascular invasion			0.319
Negative	6 (100)	31 (70)	
Positive	0 (0)	13 (30)	

Numbers in parentheses indicate percentages

LN lymph node metastasis, *HG* histologic grade, *ER* estrogen receptor

discriminant analysis (OPLS-DA) was performed to differentiate groups with different prognostic factors. Class discrimination models were built until the cross-validated predictability value did not significantly increase to avoid over-fitting of the statistical model, which was validated by the prediction of unknown samples using a leave-one-out analysis. An a priori cut-off value of 0.5 was used to evaluate the prediction results. Signals contributing to group discrimination were identified by an S-plot, and corresponding HR MAS MR spectral data were identified using Chenomx software.

3 Results

3.1 Histopathological Analysis

Tissue samples from 50 patients (mean 46 years, range 24–68 years) treated at our hospital from July 2009 to May 2011 were enrolled in this study. By pathological analyses, tumor sizes ranged from 1.3 to 11.0 cm and the mean size was 2.9 cm. A total of 26 patients (52 %) underwent modified radical mastectomy and 24 (48 %) underwent breast-conserving surgery. Pathology revealed invasive ductal carcinoma in 45 (90 %) patients, invasive lobular carcinoma in 2 (4 %) patients, mucinous carcinoma in 2 (4 %) patients, and micropapillary carcinoma in 1 (2 %) patient. The clinicopathological characteristics of our 50 sample tumors are summarized in Table 1. The mean follow-up duration was 53 months (range 43–65 months). The histological grade and p53 status showed significant differences between indolent and non-indolent tumors ($P = 0.023$, respectively). Other measured parameters were not significantly different between the two groups ($P > 0.05$).

A total of 6 (12 %) indolent tumors and 44 (88 %) non-indolent tumors were included in our present analysis, and we evaluated recurrences of less than 5 years. There were 8 (16 %) tumors with recurrence and 42 (84 %) without recurrence. Lymph node metastasis was present in 28 (56 %) and absent in 22 (44 %) tumors. There were 23 (46 %) ER-positive tumors with low HG and 11 (22 %) node-negative, ER-positive tumors with low HG. Among ER-positive tumors ($n = 34$), there were 15 (44 %) tumors without LN metastasis and 19 (56 %) with LN metastasis.

3.2 Ex Vivo HR MAS MR Spectral Analysis

Analysis of HR MAS MR spectra identified and quantified various metabolites in 50 samples. The mean values and standard deviation of choline were 8.31 ± 7.54 mM (range 0.20–36.65). On univariate analysis, the metabolites showed no significant difference between indolent and non-indolent tumors ($P > 0.05$; Table 2; Fig. 2a). Tumors without recurrence showed significantly higher Tau and Cr values than those with recurrence (Table 2; Fig. 2b). In addition, Leu was significantly higher in ER-positive tumors with lymph node metastasis than in those without lymph node metastasis ($P = 0.049$; Table 3). There were no significant differences amongst any

Table 2 Comparison of marker metabolites on ex vivo HR MAS MRS and in vivo MRS that contributed to classifying indolent breast tumors, breast tumors with recurrence, and LN metastases

	Indolent tumor		*P* value	Recurrence		*P* value	LN metastasis		*P* value
	Yes ($n = 6$)	No ($n = 44$)		Negative ($n = 42$)	Positive ($n = 8$)		Negative ($n = 28$)	Positive ($n = 22$)	
tCho PI	1.37 (9.99)	2.22 (13.58)	0.721	2.52 (16.13)	0.15 (4.84)	0.043*	2.44 (16.96)	1.41 (8.21)	0.500
tCho SNR	1.83 (3.52)	2.28 (4.08)	0.638	2.24 (4.35)	1.26 (2.85)	0.257	1.90 (3.60)	2.52 (4.60)	0.500
tCho conc.	0.00 (0.00)	0.97 (2.80)	0.530	0.97 (2.53)	0.00 (0.00)	0.035*	0.51 (2.43)	1.59 (4.15)	0.667
Creatine	6.22 (14.86)	3.49 (2.91)	0.370	3.81 (3.40)	1.37 (3.50)	0.041*	4.04 (5.08)	3.23 (2.66)	0.860
Choline	2.62 (5.55)	2.18 (2.41)	0.905	2.18 (2.40)	2.37 (3.00)	0.612	2.12 (3.74)	2.19 (2.23)	0.681
Glycine	21.46 (31.79)	13.29 (17.88)	0.474	14.30 (16.70)	11.97 (28.08)	0.490	16.41 (20.49)	11.47 (13.83)	0.506
Isoleucine	2.70 (5.04)	2.24 (3.01)	0.881	2.24 (3.52)	2.46 (7.71)	0.726	2.55 (3.95)	2.03 (2.32)	0.369
Lactate	104.7 (188.3)	75.68 (94.27)	0.387	75.68 (65.00)	135.5 (140.9)	0.612	87.50 (117.6)	65.51 (75.57)	0.309
Leucine	6.62 (7.26)	5.28 (5.59)	0.654	5.41 (5.31)	5.25 (9.05)	0.928	5.48 (6.08)	4.90 (5.30)	0.532
Methionine	1.06 (1.89)	0.62 (0.58)	0.858	0.62 (0.61)	0.56 (1.11)	0.490	0.73 (1.27)	0.52 (0.52)	0.249
O-PC	2.09 (11.49)	2.49 (3.32)	0.976	2.47 (3.39)	2.38 (4.46)	0.928	2.27 (2.59)	2.49 (4.77)	0.401
Sn-GPC	3.29 (2.94)	1.27 (2.19)	0.089	1.41 (2.70)	1.12 (2.91)	0.474	1.54 (3.29)	1.19 (2.09)	0.558
Taurine	10.88 (33.69)	12.03 (11.93)	0.788	13.27 (11.01)	6.43 (9.66)	0.041*	13.27 (10.60)	11.53 (14.61)	1.000
Valine	6.26 (8.84)	2.75 (2.68)	0.403	2.75 (2.67)	2.37 (5.41)	0.576	2.61 (3.74)	2.84 (3.07)	0.611

Data represent mean values and numbers in parentheses show standard errors. Significant differences for which $P < 0.05$ are marked by an asterisk

tCho total choline-containing compound, *PI* peak integral (AU), *SNR* signal-to-noise ratio, *LNM* lymph node metastasis, *conc.* concentration (mmol/kg), *O-PC* *O*-phosphocholine, *sn-GPC* sn-glycero-phosphocholine

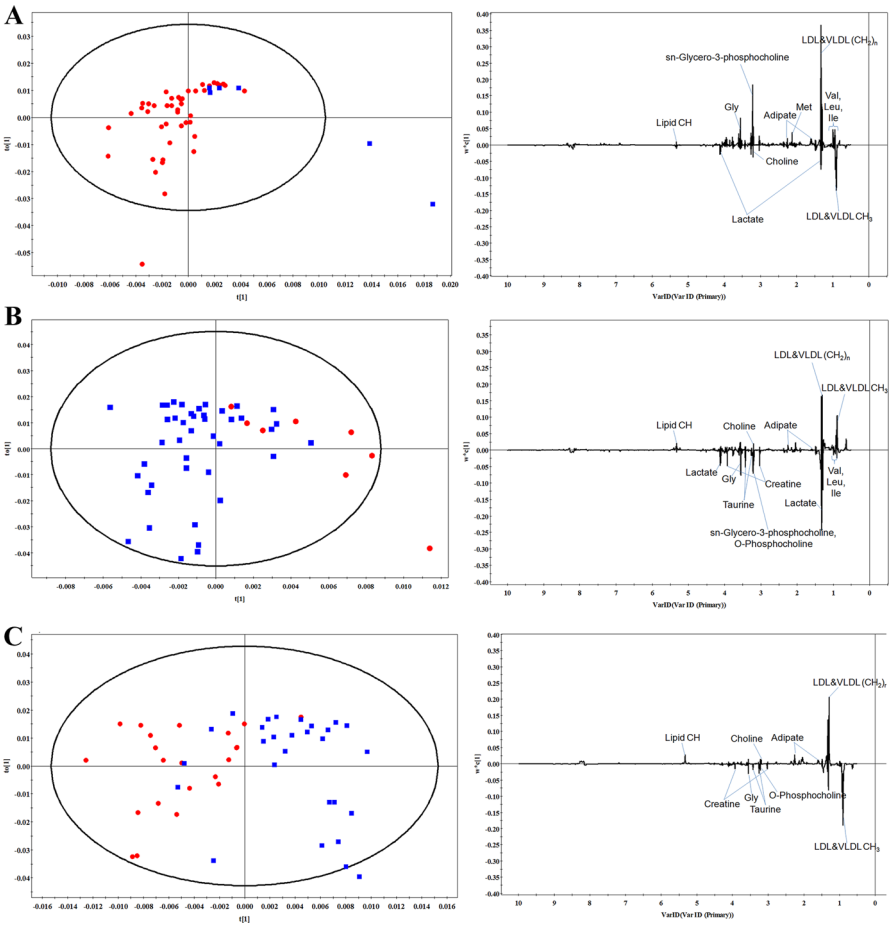

Fig. 2 Orthogonal projections to latent structure-discriminant analysis (OPLS-DA) score plots and loading plots for the prediction of indolent breast tumors (**a**), breast tumors with recurrence (**b**), and lymph node metastases (**c**)

metabolite for the prediction of node-negative, ER-positive tumors with low HG and ER-positive tumors with low HG (Table 3).

On multivariate analysis, OPLS-DA separation models were built with the HR MAS MR spectral data to predict indolent tumors, tumors with early recurrence (less than 5 years), and lymph node metastasis (Table 2; Fig. 2). The OPLS-DA loading plots showed that samples were separated and showed visible discrimination between indolent and non-indolent tumors, tumors with and without recurrence, and tumors with and without lymph node metastasis, although there were some samples that crossed over the reference line (Fig. 2). The OPLS-DA model for predicting indolent tumors demonstrated a sensitivity of 100 % and a specificity of 68 % (Table 4). The corresponding loading plot demonstrated the marker metabolites that were responsible for the separation of indolent and non-indolent tumors.

Table 3 Comparison of marker metabolites on ex vivo HR MAS MRS and in vivo MRS that contributed to the classification of ER-positive breast tumors according to the histological grade and lymph node metastases

	ER-positive, low HG		*P* value	Node-negative, ER (+), low HG		*P* value	ER-positive tumor		*P* value
	Yes ($n = 23$)	No ($n = 27$)		Yes ($n = 11$)	No ($n = 39$)		LNM (−) ($n = 14$)	LNM (+) ($n = 19$)	
tCho PI	0.41 (7.79)	2.72 (16.21)	0.352	0.39 (7.79)	2.37 (14.85)	0.490	3.73 (20.42)	0.91 (7.09)	0.313
tCho SNR	1.82 (2.92)	2.90 (4.69)	0.222	0.23 (1.95)	2.64 (4.31)	0.105	1.83 (3.07)	2.38 (4.05)	0.877
tCho conc.	0.00 (2.63)	1.50 (3.52)	0.416	0.00 (2.43)	1.50 (4.02)	0.312	1.47 (3.22)	1.95 (4.27)	1.000
Creatine	4.18 (4.14)	3.16 (3.04)	0.136	4.18 (3.47)	3.30 (3.24)	0.297	3.53 (3.82)	4.13 (5.77)	0.971
Choline	1.99 (2.87)	2.18 (2.08)	0.690	3.71 (6.24)	2.18 (2.37)	0.367	2.18 (2.13)	2.88 (5.20)	0.512
Glycine	16.89 (15.91)	11.05 (18.13)	0.355	18.16 (19.37)	11.90 (18.33)	0.131	11.90 (15.46)	17.53 (19.08)	0.402
Isoleucine	2.37 (4.43)	2.12 (2.45)	0.355	2.73 (4.04)	2.12 (2.33)	0.297	2.12 (2.09)	3.09 (3.96)	0.216
Lactate	90.01 (118.7)	73.21 (73.54)	0.335	118.1 (117.0)	69.78 (73.54)	0.059	62.44 (97.51)	106.9 (118.8)	0.135
Leucine	5.89 (6.69)	5.24 (4.20)	0.647	8.03 (12.29)	4.39 (5.25)	0.085	5.51 (5.42)	8.29 (11.60)	0.049*
Methionine	0.78 (1.37)	0.50 (0.48)	0.202	1.07 (1.87)	0.52 (0.49)	0.104	0.51 (0.59)	0.98 (1.59)	0.101
O-PC	2.48 (3.43)	2.08 (3.49)	0.853	2.46 (3.43)	2.48 (3.49)	0.972	3.11 (5.52)	2.10 (3.60)	0.308
sn-GPC	1.71 (2.83)	1.33 (2.86)	0.793	2.02 (2.86)	1.22 (2.18)	0.367	1.02 (2.18)	1.87 (2.69)	0.362
Taurine	14.19 (19.38)	9.32 (9.99)	0.113	16.20 (22.37)	11.08 (10.43)	0.081	11.39 (12.13)	15.20 (19.98)	0.402
Valine	2.45 (8.60)	2.81 (2.28)	0.778	4.00 (8.55)	2.69 (2.57)	0.143	2.87 (4.06)	4.43 (8.60)	0.216

Data represent median values and numbers in parentheses show interquartile ranges. Significant differences for which $P < 0.05$ are marked by an asterisk

tCho total choline-containing compound, *PI* peak integral (AU), *SNR* signal-to-noise ratio, *LNM* lymph node metastasis, *conc.* concentration (mmol/kg), *O-PC* *O*-phosphocholine, *sn-GPC* sn-glycero-phosphocholine

Table 4 Diagnostic performance of OPLS-DA for the prediction of indolent breast tumors, breast tumors with recurrence, and LN metastasis, and for the prediction of ER-positive breast tumors according to the histological grade and lymph node metastasis

	Indolent tumor	Recurrence	LN metastasis
Sensitivity (%)	100	77	82
Specificity (%)	68	100	96
	ER-positive tumor with low HG	LN-negative, ER-positive tumor with low HG	ER-positive tumor with LN metastasis[a]
Sensitivity (%)	96	91	93
Specificity (%)	63	64	84

ER estrogen receptor, *HG* histological grade, *LN* lymph node

[a] Included only ER-positive tumors ($n = 34$)

Indolent tumors showed elevated levels of Gly, GPC, Met, Val, Ile, and Leu, while non-indolent tumors showed elevated levels of Lac and Cho (Fig. 2a). However, these metabolite did not show significant differences between indolent and non-indolent tumors on univariate analysis (Table 2).

The OPLS-DA model for the prediction of tumors with early recurrence showed a sensitivity of 77 % and a specificity of 100 % (Table 4). The loading plot demonstrated the marker metabolites that were responsible for the separation of tumors with and without early recurrence (Fig. 2b). Tumors without recurrence showed elevated levels of Gly, Lac, Cr, Tau, GPC, and PC, while tumors with recurrence showed elevated levels of Cho (Fig. 2b). Among the marker metabolites responsible for the separation, the levels of Cr and Tau significantly elevated in tumors without recurrence (Table 2).

When we compared tumors with and without lymph node metastasis, the OPLS-DA model showed a good separation with a sensitivity of 82 % and a specificity of 96 % (Table 4). Tumors with lymph node metastasis showed elevated levels of Gly, Cr, Tau, and PC, whereas tumors without LN metastasis showed a elevated levels ofCho (Fig. 2c).

3.3 ER-Positive Tumors

We classified ER-positive tumors into three different groups based on the histologic grade and lymph node metastasis as follows: (1) ER-positive tumors with low HG vs. others; (2) node-negative, ER-positive tumors with low HG vs. others; and (3) ER-positive tumors with LN metastasis vs. those without LN metastasis. The diagnostic performance for the prediction of ER-positive tumors with low HG showed a sensitivity of 96 % and a specificity of 63 %, respectively (Table 4). The loading plot demonstrated elevated levels of Cr and GPC in ER-positve tumors with low HG and, while other tumors showed elevated levels of Gly, Lac, Cho, and PC (Fig. 3a), which were not significantly different between two groups on univariate analysis (Table 3).

The diagnostic performance for the prediction of node-negative, ER-positive tumors with low HG showed sensitivity of 91 % and specificity of 64 %. The loading plot demonstrated elevated levels of Met, Val, Ile, and Leu, while other tumors showed elevated levels of Gly, Cr, Tau, and Cho (Fig. 3b), which did not show significant differences on univariate analysis (Table 3). When we divided ER-positive tumors into two groups according to the status of lymph node metastasis, the OPLS-DA model showed a sensitivity of 93 % and a specificity of 84 %, respectively (Table 4). Based on the loading plot (Fig. 3c), ER-positive tumors with lymph node metastasis showed elevated levels of Gly, Cr, Tau, GPC, and PC, which did not show significant difference (Table 3).

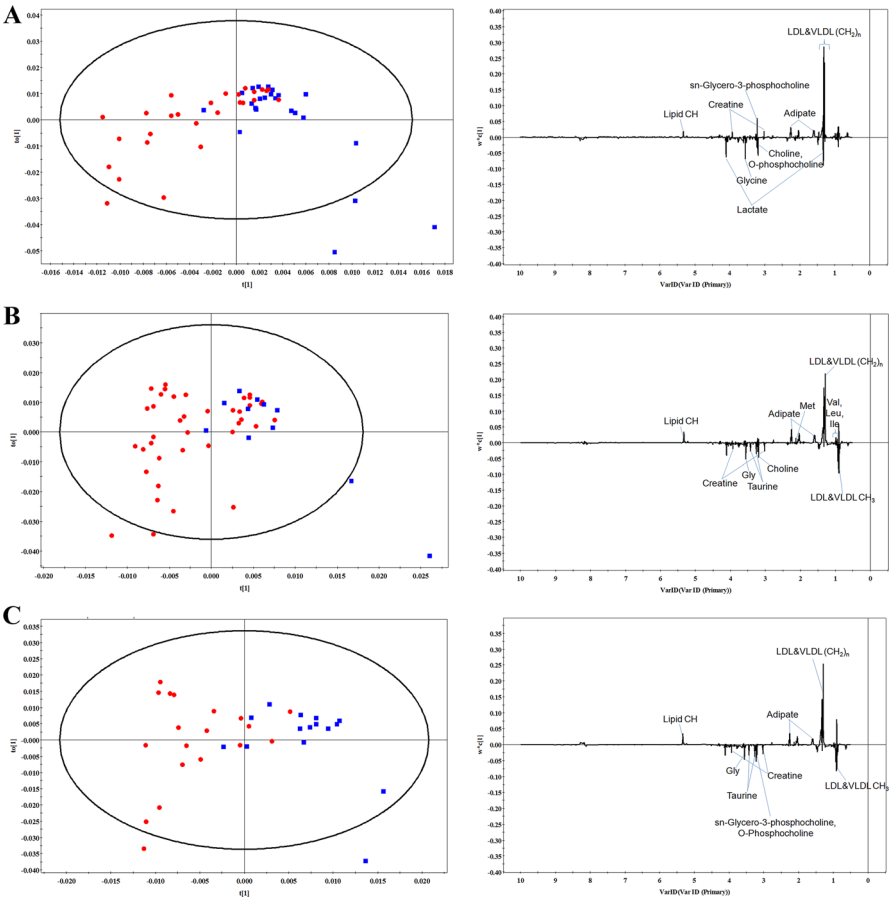

Fig. 3 Orthogonal projections to latent structure-discriminant analysis (OPLS-DA) score plots and loading plots for the prediction of ER-positive breast tumors with a low histological grade (**a**), node-negative, ER-positive breast tumors with a low histological grade (**b**), and ER-positive breast tumors with lymph node metastases (**c**)

3.4 In Vivo MR Spectroscopic Analysis

On univariate analysis, tumors without recurrence showed significantly higher levels of the tCho peak integral and absolute tCho concentrations compared to those with recurrence ($P = 0.043$ and 0.035, respectively) (Table 2). Non-indolent tumors and tumors with lymph node metastasis showed elevated levels of tCho SNR and tCho concentration, although they did not reach statistical significance (Table 2). In addition, we found no significant differences in the in vivo MR spectroscopic parameters for the prediction of ER-positive tumors according to HG or lymph node metastasis status (Tables 2, 3).

4 Discussion

Breast cancer is a complex disease with various prognostic implications. In our current study, we demonstrate the possibility of differentiating patients with recurrence from those without recurrence, in addition to differentiating indolent tumors from non-indolent tumors with high sensitivity and specificity based on metabolic profiling using ex vivo HR MAS MRS and in vivo MRS. MR metabolomics using HR MAS MRS and in vivo MRS could thus be utilized to predict the prognosis in breast cancer patients. The detection of biological markers that have prognostic significance could guide personalized treatments of breast cancer, and might also yield a better understanding of the processes underlying cancer progression [4]. The metabolic data contained in the spectra can be used to establish prognostic and predictive classifications using appropriate multivariate statistical analyses, such as principal component analysis (PCA) and OPLS-DA, which can handle the highly co-variant nature of MRS variables [10, 25]. The MR metabolic profile of a tissue sample contains information related to breast cancer subtypes [26, 27]. Giskeødegård et al. reported that the metabolic profiles obtained using HR MAS MRS contain prognostic information that extends beyond that of traditional clinical parameters, with high levels of lactate and glycine indicative of a lower 5-year survival rate [4]. Several studies have reported that the MR metabolic profile contains data related to hormone receptor status and lymphatic spread [8, 11, 26]. The results of our present study concur with those of previous reports [4, 8, 11, 26], in which Lac was found to be increased in non-indolent tumors and Gly was increased in tumors with lymph node metastasis and recurrence. In addition, Tau and Cr were also found to be increased in tumors with lymph node metastasis and recurrence. However, our present data did not reach our threshold for statistically significant differences because the sample size was relatively small. We have proposed and agreed with the theory that highly aggressive cancer cells might cause high glucose uptake and increased lactate production [3, 4].

Giskeødegård et al. [4] reported previously that visual inspection of the mean spectra show different metabolite profiles between survivors and nonsurvivors, with breast cancer tissues from nonsurvivors containing larger amounts of Lac, Gly, and PC, and smaller amounts of Glu, Cr, and Tau compared with tissues from survivors. They found that higher levels of lactate and glycine were associated with a poor

prognosis, and therefore suggested that lactate and glycine represent potential biomarkers for the prediction of breast cancer prognoses. Another study by Giskeødegård et al. [13] showed that ER-positive and ER-negative tumors had different metabolic patterns. Other studies have reported that elevated levels of Lac are frequently observed in cancer compared with normal tissues under both aerobic and anaerobic conditions [4, 25]. Hypoxia is a common condition in solid tumors, which has been correlated with aggressive and metastatic tumors [4]. Under conditions with sufficient oxygen levels, cancer cells can convert glucose to lactate, a phenomenon known as the Warburg effect [28]. A preclinical study on ER-positive breast cancers reported that glucose metabolism to lactate can be enhanced by estrogen [29]. In our present study, increased levels of Lac were documented in tumors with poor prognostic indicators, in accord with previous studies of breast [4], cervical [30], lung [31], and head and neck cancers [32]. In contrast with a previous study [4], however, we here found that Lac was increased in tumors without early recurrence compared to those with recurrence. In addition, we found that tCho levels were increased in tumors without early recurrence compared to those with recurrence. We propose that a long-term follow-up study might be the best way to confirm this finding.

Previously, higher levels of Gly have been associated with a poor prognosis in ER-positive breast cancers [4]. Gly production is the major pathway for intracellular Cho metabolism in breast cancer cells [28, 33]. Perou et al. found that an increased level of Gly was present in the basal-like model, in contrast to the luminal-like model, which suggested a metabolic shift from PC synthesis to Gly formation in the basal-like subtype [34]. Potentially, increased levels of Gly in breast cancer patients with a poor prognosis result from altered Cho glycolysis and/or metabolism [4, 34].

Among molecular subtypes, triple-negative or HER2-positive tumors can recur at 2–3 years after treatment. However, luminal-type tumors with positive hormone receptor status can recur after 5 years, or in some cases even after 10 years. In our present study, we found that Gly was associated with lymph node metastasis and a high histological grade, which is consistent with the results of a previous study [4]. In addition, Tau, Cr, and Lac were also found to be increased in ER-positive tumors with lymph node metastasis or a high histological grade. This result might be useful for predicting the prognosis of these luminal types of breast cancers. In our present study also, Gly was a more predictive metabolite than Lac for ER-positive tumors. We propose that Lac on HR MAS MRS and tCho on in vivo MRS might be associated with an early recurrence of less than 5 years.

Our study had several limitations. First, it should be noted that we included a relatively small number of samples. The number of indolent tumors was 6, which was small to generalize our results. Therefore, the significance of our statistical analysis should be considered in the particular context of the preliminary study in which the number of cases presented was relatively small. Considering the many factors that can affect metabolite-dependent changes in tumors, such as the histological grade and heterogeneity of the tumor microenvironment, further studies with a larger number of samples will be needed to confirm our present findings. Second, although different metabolite profiles that could separate tumors with different prognoses were identified, we were not able to determine the importance of

each metabolite. For a detailed characterization and description of the significance of metabolite differences in tumors, additional studies combined with known prognostic factors, including genetic and proteomic data, will be needed. Third, as we included only parts of whole breast tumors, our data might not reflect ongoing metabolic alterations in entire tumors because of the intrinsically heterogeneous nature of breast tumors. The direct application of our result to clinical setting is limited. However, it is the first study to evaluate the role of in vivo MRS in addition to HR MAS MRS in breast cancer, especially in ER-positive breast cancers. Further studies with larger numbers of samples are needed to validate our multivariate classification models.

In conclusion, our current data suggest that several metabolites of Gly, Lac, Tau, Cr, GPC, and Cho on HR MAS MRS and tCho on in vivo MRS could represent candidate biomarkers for predicting indolent breast tumors, breast tumors with early recurrence, and lymph node metastasis. In the OPLS-DA model of metabolite profiles, patients with ER-positive tumors could be separated into two distinct groups with different prognosis based on the histological grade and lymph node metastasis. In addition, tissue samples from non-indolent tumors contained more Lac than those from indolent tumors. Therefore, metabolite profiling on HR MAS MRS and tCho on in vivo MRS might enable better predictions of the prognosis of breast cancer, especially in ER-positive breast cancer cases. Future prospective studies with a larger patient cohort will be needed to confirm these findings.

Acknowledgments The biospecimens and data used in this study were provided by the Asan Bio-Resource Center, Korea Biobank Network (2011-7(36)).

References

1. C.M. Perou, A.L. Børresen-Dale, Cold Spring Harb. Perspect. Biol. (2011). doi:10.1101/cshperspect.a003293
2. J. Ferlay, D.M. Parkin, E. Steliarova-Foucher, Eur. J. Cancer **46**, 765–781 (2010)
3. D. Hanahan, R.A. Weinberg, Cell **144**, 646–674 (2011)
4. G.F. Giskeødegård, S. Lundgren, B. Sitter, H.E. Fjøsne, G. Postma, L.M. Buydens, I.S. Gribbestad, T.F. Bathen, NMR Biomed. **25**, 1271–1279 (2012)
5. S. Moestue, B. Sitter, T.F. Bathen, M.B. Tessem, I.S. Gribbestad, Curr. Top. Med. Chem. **11**, 2–26 (2011)
6. P.J. Bolan, M.T. Nelson, D. Yee, M. Garwood, Breast Cancer Res. **7**, 149–152 (2005)
7. J.S. Choi, H.M. Baek, S. Kim, M.J. Kim, J.H. Youk, H.J. Moon, E.K. Kim, Y.K. Nam, PLoS One **8**, e83866 (2013). doi:10.1371/journal.pone.0083866
8. B. Sitter, U. Sonnewald, M. Spraul, H.E. Fjösne, I.S. Gribbestad, NMR Biomed. **15**, 327–337 (2002)
9. B. Sitter, S. Lundgren, T.F. Bathen, J. Halgunset, H.E. Fjosne, I.S. Gribbestad, NMR Biomed. **19**, 30–40 (2006)
10. T.F. Bathen, B. Sitter, T.E. Sjøbakk, M.B. Tessem, I.S. Gribbestad, Cancer Res. **70**, 6692–6696 (2010)
11. G.F. Giskeødegård, M.T. Grinde, B. Sitter, D.E. Axelson, S. Lundgren, H.E. Fjøsne, S. Dahl, I.S. Gribbestad, T.F. Bathen, J. Proteome Res. **9**, 972–979 (2010)
12. I.S. Gribbestad, T.E. Singstad, G. Nilsen, H.E. Fjøsne, T. Engan, O.A. Haugen, P.A. Rinck, J. Magn. Reson. Imaging **8**, 1191–1197 (1998)
13. L. Bartella, E.A. Morris, D.D. Dershaw, L. Liberman, S.B. Thakur, C. Moskowitz, J. Guido, W. Huang, Radiology **239**, 686–692 (2006)
14. P.A. Baltzer, M. Dietzel, Radiology **267**, 735–746 (2013)
15. D.K. Yeung, W.T. Yang, G.M. Tse, Radiology **225**, 190–197 (2002)

16. H.J. Shin, H.M. Baek, J.H. Cha, H.H. Kim, AJR Am. J. Roentgenol. **198**, W488–W497 (2012)
17. E. Montagna, V. Bagnardi, N. Rotmensz, G. Viale, G. Cancello, M. Mazza, A. Cardillo, R. Ghisini, V. Galimberti, P. Veronesi, S. Monti, A. Luini, P.R. Raviele, M.G. Mastropasqua, A. Goldhirsch, M. Colleoni, Breast Cancer Res. Treat. **129**, 867–875 (2011)
18. J.J. de Ronde, J. Hannemann, H. Halfwerk, L. Mulder, M.E. Straver, M.K. Vrancken Peeters, J. Wesseling, M. van de Vijver, L.F. Wessels, S. Rodenhuis, Breast Cancer Res. Treat. **119**, 119–126 (2010)
19. M.C. Cheang, S.K. Chia, D. Voduc, D. Gao, S. Leung, J. Snider, M. Watson, S. Davies, P.S. Bernard, J.S. Parker, C.M. Perou, M.K. Ellis, T.O. Nielsen, Breast Cancer Inst. **101**, 736–750 (2009)
20. A. Goldhirsch, W.C. Wood, A.S. Coates, R.D. Gelber, B. Thurlimann, H.J. Senn; Panel members, Ann. Oncol. **22**, 1736–1747 (2011)
21. J.A. Sparano, S. Paik, J. Clin. Oncol. **26**, 721–728 (2008)
22. S. Paik, G. Tang, S. Shak, C. Kim, J. Baker, W. Kim, M. Cronin, F.L. Baehner, D. Watson, J. Bryant, J.P. Costantino, C.E. Jr Geyer, D.L. Wickerham, N. Wolmark, J. Clin. Oncol. **24**, 3726–3734 (2006)
23. D.C. Allred, J.M. Harvey, M. Berardo, G.M. Clark, Mod. Pathol. **11**, 155–168 (1998)
24. A. Naressi, C. Couturier, J.M. Devos, M. Janssen, C. Mangeat, R. de Beer, D. Graveron-Demilly, MAGMA **12**, 141–152 (2001)
25. T.F. Bathen, B. Geurts, B. Sitter, H.E. Fjøsne, S. Lundgren, L.M. Buydens, I.S. Gribbestad, G. Postma, G.F. Giskeødegård, PLoS One **8**, e61578 (2013). doi:10.1371/journal.pone.0061578
26. S.A. Moestue, E. Borgan, E.M. Huuse, E.M. Lindholm, B. Sitter, A.L. Børresen-Dale, O. Engebraaten, G.M. Maelandsmo, I.S. Gribbestad, BMC Cancer **10**, 433 (2010)
27. B. Sitter, T.F. Bathen, T.E. Singstad, H.E. Fjøsne, S. Lundgren, J. Halgunset, I.S. Gribbestad, NMR Biomed. **23**, 424–431 (2010)
28. O. Warburg, Science **123**, 309–314 (1956)
29. D. Rivenzon-Segal, S. Boldin-Adamsky, D. Seger, R. Seger, H. Degani, Int. J. Cancer **107**, 177–182 (2003)
30. S. Walenta, M. Wetterling, M. Lehrke, G. Schwickert, K. Sundfør, E.K. Rofstad, W. Mueller-Klieser, Cancer Res. **60**, 916–921 (2000)
31. H. Yokota, J. Guo, M. Matoba, K. Higashi, H. Tonami, Y. Nagao, J. Magn. Reson. Imaging **25**, 992–999 (2007)
32. D.M. Brizel, T. Schroeder, R.L. Scher, S. Walenta, R.W. Clough, M.W. Dewhirst, W. Mueller-Klieser, Int. J. Radiat. Oncol. Biol. Phys. **51**, 349–353 (2001)
33. R. Katz-Brull, D. Seger, D. Rivenson-Segal, E. Rushkin, H. Degani, Cancer Res. **62**, 1966–1970 (2002)
34. C.M. Perou, T. Sørlie, M.B. Eisen, M. van de Rijn, S.S. Jeffrey, C.A. Rees, J.R. Pollack, D.T. Ross, H. Johnsen, L.A. Akslen, O. Fluge, A. Pergamenschikov, C. Williams, S.X. Zhu, P.E. Lønning, A.L. Børresen-Dale, P.O. Brown, D. Botstein, Nature **406**, 747–752 (2000)